Interaction of Urea with a Hydroxide-Bridged Dinuclear Nickel Center: An Alternative Model for the Mechanism of Urease

Amy M. Barrios and Stephen J. Lippard*

Contribution from the Department of Chemistry, Massachusetts Institute of Technology, Cambridge, Massachusetts 02139

Received January 18, 2000

Abstract: A hydroxide-bridged dinuclear nickel complex with a urea molecule linking the two metal ions through its carbonyl oxygen atom has been prepared as a model for the metalloenzyme urease. This complex, $[Ni_2(\mu\text{-OH})(\mu\text{-urea})(bdptz)(urea)(CH_3CN)](ClO_4)_3$, where bdptz is the dinucleating ligand 1,4-bis(2,2′-dipyridylmethyl)phthalazine, effects the hydrolysis of urea upon heating in a two-step reaction. In the first step, a molecule of ammonia is eliminated from urea with concomitant production of cyanate, the first-order rate constant in acetonitrile being $(7.7 \pm 0.5) \times 10^{-4}$ h^{-1}. This reaction is at least 500 times faster than the spontaneous decomposition of urea under the same conditions. When the cyanate-containing product is further heated in the presence of water, the cyanate is hydrolyzed with a second-order rate constant of $(9.5 \pm 1) \times 10^{-4}$ M^{-1} h^{-1}. Reaction of $[Ni_2(\mu\text{-OH})(\mu\text{-urea})(bdptz)(urea)(CH_3CN)](ClO_4)_3$ in 50% aqueous acetonitrile afforded ammonia with no appreciable buildup of the cyanate-containing species. A possible analogue of the cyanate-containing product, $[Ni_2(\mu\text{-OH})(\mu\text{-}H_2O)(bdptz)(\mu\text{-OCN})]_2(OTs)_4$, was independently synthesized and structurally characterized. These results establish the precedence for hydrolysis of urea via a cyanate intermediate as an alternative mechanism for the urease-catalyzed hydrolysis of urea.

Introduction

The metalloenzyme urease holds a distinguished place in the history of enzymology.[1] First crystallized in 1926,[2] the nickel dependence of urease was not recognized until nearly 50 years later.[3] Urease is the only metallohydrolase that utilizes nickel, and a detailed picture of its active site has emerged over the past several years through X-ray crystallographic studies of the enzyme isolated from different sources.[4−8] A schematic view of the dinickel center in urease from *Klebsiella aerogenes* is shown in Figure 1. Each nickel ion is coordinated to two histidine residues from the protein, and a carbamylated lysine residue bridges the two metal ions. The second nickel ion is additionally ligated by an aspartate residue. Two terminally coordinated water molecules and one bridging water molecule or hydroxide ion complete the coordination spheres of the metal ions, resulting in a distorted square pyramidal environment for Ni(1) and a pseudooctahedral ligand environment for Ni(2).

The reaction catalyzed by the dinickel site in urease is the hydrolysis of urea to form ammonia and carbon dioxide.[9] The hydrolysis of urea is not a trivial task; the uncatalyzed reaction has never been observed.[10] In aqueous solutions, urea spontaneously eliminates ammonia to form cyanic acid, in a reaction that is pH independent from pH 2 to 12, with a half-life of 3.6 years at 38 °C.[10] The stability of urea is attributed to its resonance energy, which has been estimated at 30−40 kcal/mol.[11] Urease converts urea to products at a rate at least 10^{14} times faster than the spontaneous decomposition rate.[10] The proposed mechanism of urea hydrolysis at the active site of the enzyme, shown in Scheme 1, involves (i) production of a hydroxide ion at the dinickel(II) center, (ii) activation of the substrate by coordination to one or both metal ions, and (iii) nucleophilic attack of the hydroxide ion at the carbonyl carbon atom of the substrate, producing ammonia and carbamic acid, which spontaneously decompose to form a second equivalent of ammonia and carbon dioxide. Carbamate is the first species released from the enzyme,[12] but there is no direct evidence that it is the first intermediate formed in the reaction.

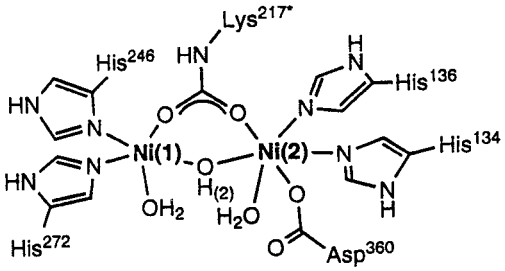

Figure 1. Schematic view of the active site of urease from *K. aerogenes*.[4]

(1) Lippard, S. J. *Science* **1995**, *268*, 996−997.
(2) Sumner, J. B. *J. Biol. Chem.* **1926**, *69*, 435−441.
(3) Dixon, N. E.; Gazzola, C.; Blakeley, R. L.; Zerner, B. *J. Am. Chem. Soc.* **1975**, *97*, 7, 4131−4132.
(4) Jabri, E.; Carr, M. B.; Hausinger, R. P.; Karplus, P. A. *Science* **1995**, *268*, 998−1004.
(5) Pearson, M. A.; Michel, L. O.; Hausinger, R. P.; Karplus, P. A. *Biochemistry* **1997**, *36*, 8164−8172.
(6) Benini, S.; Rypniewski, W. R.; Wilson, K. S.; Ciurli, S.; Mangani, S. *JBIC* **1998**, *3*, 268−273.
(7) Benini, S.; Rypniewski, W. R.; Wilson, K. S.; Miletti, S.; Ciurli, S.; Mangani, S. *Structure* **1999**, *7*, 205−216.
(8) Benini, S.; Rypniewski, W. R.; Wilson, K. S.; Miletti, S.; Ciurli, S.; Mangani, S. *JBIC* **2000**, *5*, 110−118.
(9) (a) Fearon, W. R. *Biochem. J.* **1923**, *17*, 84−93. (b) Mack, E.; Villars, D. S. *J. Am. Chem. Soc.* **1923**, *45*, 505−510. (c) Karplus, P. A.; Pearson, M. A.; Hausinger, R. P. *Acc. Chem. Res.* **1997**, *30*, 330−337.
(10) Blakeley, R. L.; Treston, A.; Andrews, R. K.; Zerner, B. *J. Am. Chem. Soc.* **1982**, *104*, 612−614.
(11) Wheland, G. W. *Resonance in Organic Chemistry*; Wiley: New York, 1955.
(12) Blakeley, R. L.; Hinds, J. A.; Kunze, H. E.; Webb, E. C.; Zerner, B. *Biochemistry* **1969**, *5*, 1991−2000.

10.1021/ja000202v CCC: $19.00
Published on Web 09/07/2000

Scheme 1

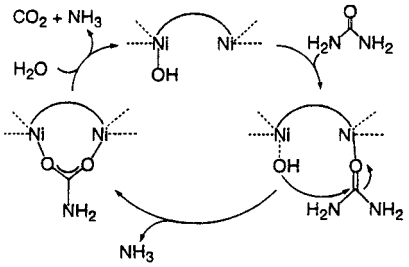

A number of researchers have reported the synthesis of dinuclear nickel complexes of relevance to the active site of urease.[13−19] Several of these model complexes have a urea molecule bound to the dinickel center.[20−22] In all but one case, the urea molecule binds through its carbonyl oxygen atom to one of the nickel ions in the complex; this coordination mode is likely to occur in the enzyme. In addition to these structural models, a few of the complexes reported in the literature show reactivity pertinent to that of urease. Ethanolysis of urea at a dinickel center[10,23,24] presumably takes place via nucleophilic attack of ethanol solvent on coordinated urea. Complexes that promote the elimination of ammonia from a coordinated urea to form cyanates are also known,[25−27] although the further reactivity of the resulting dinickel cyanate compounds was not investigated.

The fact that no dinuclear nickel complex reported thus far has proved capable of hydrolyzing urea to ammonia and carbon dioxide provides an intriguing challenge to the synthetic bioinorganic chemist. The design of a complex that can produce a sufficiently nucleophilic hydroxide ion and at the same time activate a urea molecule by coordination to one or both metal ions should facilitate the successful hydrolysis of urea under the right conditions. To this end, we recently reported a dinuclear nickel complex, $[Ni_2(\mu\text{-}OH)(\mu\text{-}H_2O)(bdptz)(H_2O)_2](OTs)_3$ (where bdptz is the dinucleating ligand 1,4-bis(2,2′-dipyridylmethyl)-phthalazine), that is capable of hydrolyzing a bound amide substrate by intramolecular attack of a coordinated hydroxide ion.[28] On the basis of the results of this study, this complex seemed a likely candidate to effect the hydrolysis of urea. In the present report we describe the synthesis of a related dinuclear nickel complex containing a unique bridging urea molecule. Upon heating, this complex effects the hydrolysis of urea by a pathway involving cyanate ion that is distinct from that previously proposed for the enzyme. These results provide the first direct evidence for a mechanism long considered as an alternative for the enzymatic hydrolysis of urea.[9a,b]

Experimental Section

General Considerations. All reagents were obtained from commercially available sources and used without further purification, unless otherwise noted. The ligand 1,4-bis(2,2′-dipyridylmethyl)phthalazine was prepared as previously described.[28] The complexes $[Ni(terpy)(H_2O)_3](OTs)_2$ and $[Ni_2(\mu\text{-}OH)(\mu\text{-}H_2O)(bdptz)(H_2O)_2](OTs)_3$ were prepared according to published procedures.[28] Fourier transform infrared spectra were recorded on a Bio-Rad FTS-135 instrument, and UV−vis spectra were obtained by using a Hewlett-Packard 8453-A diode array spectrophotometer.

CAUTION: The syntheses and procedures described below involve compounds that contain the perchlorate ion, which can detonate explosively and without warning. Although we have not encountered any problems with the reported compounds, all due precautions should be taken.

$[Ni_2(\mu\text{-}OH)(\mu\text{-}H_2O)(bdptz)(urea)_2](ClO_4)_3$ (1). A 52.8 mg, 144 μmol portion of $[Ni(H_2O)_6](ClO_4)_2$ was dissolved in 1.5 mL of methanol with stirring. A 33.4 mg, 71.5 μmol portion of bdptz was added as a solid to the methanolic nickel solution. After the mixture was allowed to stir for 2−3 min, 1 equiv of an aqueous 1 M NaOH solution was added, followed by 10 equiv of urea. Diffusion of diethyl ether vapor into the resulting brown methanolic solution resulted in X-ray quality brown-purple crystals of **1** (61 mg, 82% yield). UV−vis (CH_3OH) (λ_{max}, nm (ϵ, $M^{-1}cm^{-1}$)): 562 (66), 770 (50), 940 (62). FTIR (KBr, cm^{-1}): 3380 (s, br), 2982 (w), 1663 (s), 1609 (s), 1576 (s), 1477 (s), 1445 (s), 1373 (m), 1005 (s, br), 771 (m), 630 (m). Anal. Calcd for **1**, $Ni_2Cl_3C_{32}H_{33}N_{10}O_{16}$: C, 37.05; H, 3.21; N, 13.50. Found: C, 37.52; H, 3.53; N, 13.26.

$[Ni_2(\mu\text{-}OH)(\mu\text{-urea})(bdptz)(urea)(CH_3CN)](ClO_4)_3$ (2). A 55.9 mg, 153 μmol portion of $[Ni(H_2O)_6](ClO_4)_2$ was dissolved in 2 mL of acetonitrile with stirring. To this solution, 35.3 mg, 75.6 μmol of bdptz was added as a solid, portionwise. The mixture was allowed to stir until all of the ligand had dissolved before 70 μL (70 μmol) of an aqueous 1 M NaOH solution was added in a dropwise fashion. Finally, 10 equiv of urea was added, and the resulting brown solution was allowed to stir for a few minutes more. A purple-brown crystalline product (60 mg, 80% yield) suitable for X-ray structure determination was isolated upon slow diffusion of diethyl ether vapor into the reaction solution. UV−vis (CH_3CN) (λ_{max}, nm (ϵ, $M^{-1}cm^{-1}$)): 549 (43), 771 (33), 940 (47). FTIR (KBr, cm^{-1}): 3400 (s, br), 1661 (s), 1637 (s), 1611 (s), 1578 (m), 1477 (m), 1450 (m), 1373 (m), 1350 (w), 1090 (br). Anal. Calcd for **2**, $Ni_2Cl_3C_{34}H_{34}N_{11}O_{15}$: C, 38.51; H, 3.23; N, 14.53. Found: C, 38.91; H, 3.65; N, 14.62.

$[Ni_2(\mu\text{-}OH)(\mu\text{-}H_2O)(bdptz)(\mu\text{-}OCN)]_2(OTs)_4$ (3). A 43.7 mg, 37.4 μmol portion of $[Ni_2(\mu\text{-}OH)(\mu\text{-}H_2O)(bdptz)(H_2O)_2](OTs)_3$ was dissolved in 2 mL of ethanol with stirring. A 1.8 mL aliquot of 20 mM NaNCO in 9:1 EtOH/H_2O was added in a dropwise fashion, resulting in a green solution. Upon slow evaporation of the resulting solution, green crystals formed (70 mg, 93% crude yield). X-ray diffraction data obtained from a single green crystal provided the structure of the compound. UV−vis (CH_3CN) (λ_{max}, nm (ϵ, $M^{-1}cm^{-1}$)): 537 (39), 785 (28), 931 (48). FTIR (KBr, cm^{-1}): 3450 (br), 3079 (w), 3044 (w), 3000 (w), 2915 (w), 2164 (vs), 1601 (s), 1572 (m), 1475 (m), 1443 (s), 1369 (w), 1184 (s), 1117 (s), 1027 (s), 1005 (s), 875 (w), 814 (w), 762 (m), 679 (m). Anal. Calcd for $\mathbf{3}\cdot 2EtOH\cdot 6H_2O$, $C_{94}H_{102}N_{14}O_{26}Ni_4S_4$: C, 51.16; H, 4.66; N, 8.89. Found: C, 51.13; H, 4.25; N, 8.53.

Collection and Reduction of X-ray Data. Procedures for the collection and reduction of X-ray data have been reported previously.[29]

(13) Chadhuri, P.; Küppers, H.-J.; Wieghardt, K.; Gehring, S.; Haase, W.; Nuber, B.; Weiss, J. *J. Chem. Soc., Dalton Trans.* **1988**, 1367−1370.
(14) Stemmler, A. J.; Kampf, J. W.; Kirk, M. L.; Pecoraro, V. L. *J. Am. Chem. Soc.* **1995**, *117*, 6368−6369.
(15) Ito, M.; Takita, Y. *Chem. Lett.* **1996**, 929−930.
(16) Volkmer, D.; Hörstmann, A.; Griesar, K.; Haase, W.; Krebs, B. *Inorg. Chem.* **1996**, *35*, 1132−1135.
(17) Volkmer, D.; Hommerich, B.; Griesar, K.; Haase, W.; Krebs, B. *Inorg. Chem.* **1996**, *35*, 3792−3803.
(18) Hosokawa, Y.; Yamane, H.; Nakao, Y.; Matsumoto, K.; Takamizawa, S.; Mori, W.; Suzuki, S. *Chem. Lett.* **1997**, 891−892.
(19) Hommerich, B.; Schwöppe, H.; Volkmer, D.; Krebs, B. *Z. Anorg. Allg. Chem.* **1999**, *625*, 75−82.
(20) Wages, H. E.; Taft, K. L.; Lippard, S. J. *Inorg. Chem.* **1993**, *32*, 4985−4987.
(21) Koga, T.; Furutachi, H.; Nakamura, T.; Fukita, N.; Ohba, M.; Takahashi, K.; Okawa, H. *Inorg. Chem.* **1998**, *37*, 989−996.
(22) Meyer, F.; Pritzkow, H. *J. Chem. Soc., Chem. Commun.* **1998**, 1555−1556.
(23) Yamaguchi, K.; Koshino, S.; Akagi, F.; Suzuki, M.; Uehara, A.; Suzuki, S. *J. Am. Chem. Soc.* **1997**, *119*, 5752−5753.
(24) Konrad, M.; Meyer, F.; Jacobi, A.; Kircher, P.; Rutsch, P.; Zsolnai, L. *Inorg. Chem.* **1999**, *38*, 4559−4566.
(25) Uozumi, S.; Furutachi, H.; Ohba, M.; Okawa, H.; Fenton, D. E.; Shindo, K.; Murata, S.; Kitko, D. J. *Inorg. Chem.* **1998**, *37*, 6281−6287.
(26) Roecker, L.; Akande, J.; Elam, L. N.; Gauga, I.; Helton, B. W.; Prewitt, M. C.; Sargeson, A. M.; Swango, J. H.; Willis, A. C.; Xin, T.; Xu, J. *Inorg. Chem.* **1999**, *38*, 1269−1275.
(27) Meyer, F.; Kaifer, E.; Kircher, P.; Heinze, K.; Pritzkow, H. *Chem.−Eur. J.* **1999**, *5*, 1617−1630.
(28) Barrios, A. M.; Lippard, S. J. *J. Am. Chem. Soc.* **1999**, *121*, 11751−11757.
(29) Feig, A. L.; Bautista, M. T.; Lippard, S. J. *Inorg. Chem.* **1996**, *35*, 6892−6898.

Table 1. Summary of X-ray Crystallographic Data

	1·2CH_3OH·2H_2O	**2**·CH_3CN·CH_3OH·$CH_3CH_2OCH_2CH_3$	**3**·6CH_3CH_2OH
formula	$C_{33}H_{43}N_{10}O_{20}Ni_2Cl_3$	$C_{42}H_{57}N_{12}O_{19}Ni_2Cl_3$	$C_{98}H_{102}N_{14}O_{22}Ni_4S_4$
fw	1123.54	1257.77	1095.51
space group	*Pnma*	*P*2(1)/*m*	*P*2(1)/*n*
a, Å	17.6122(8)	10.429(2)	13.520(14)
b, Å	21.1269(10)	21.129(4)	12.434(9)
c, Å	14.3975(7)	12.695(4)	31.21(3)
α, deg			
β, deg		106.129(14)	100.938(11)
γ, deg			
V, Å^3	5357.2(4)	2687.2(12)	5151(8)
Z	4	2	2
ρ_{calcd}, g/cm^3	1.393	1.353	1.413
T, °C	−85	−85	−85
μ(Mo Kα), mm^{-1}	0.928	0.912	0.877
2θ limits, deg	3−57	3−57	3−57
total no. of data	32874	17030	31442
no. of unique data	6609	6412	11910
observed data[a]	4243	3831	5604
no. of parameters	314	423	667
R1,[b] %	6.68	6.57	5.98
wR2,[c] %	22.50	16.58	14.29
max, min peaks, e/Å^3	0.974, −0.508	1.094, −0.765	1.063, −1.200

[a] Observation criterion: $I > 2\sigma(I)$. [b] $R1 = \Sigma||F_o| - |F_c||/\Sigma|F_o|$. [c] $wR2 = \{\Sigma[w(F_o^2 - F_c^2)^2]/\Sigma[w(F_o^2)^2]\}^{1/2}$.

The crystals were mounted on glass fibers with Paratone-N (Exxon) and cooled rapidly in the −85 °C cold stream of a Bruker CCD X-ray diffraction system controlled by a Pentium-based PC running the SMART software package.[30] The structures were solved by using the direct methods program XS, and refinements were carried out with XL. Both programs are part of the SHELXTL program package.[31] All non-hydrogen atoms were refined by a series of least squares cycles. Hydrogen atoms were assigned idealized positions and given a thermal parameter 1.2 times that of the atom to which they are attached. Empirical absorption corrections were calculated and applied for each structure with SADABS,[32] and PLATON[33] was used to search for higher symmetry.

The structure of **2** has disorder in the two terminal ligands of the dinuclear nickel complex. There is a crystallographically imposed mirror plane running through the molecule, bisecting the Ni—Ni vector perpendicular to the plane of the phthalazine rings. The terminal coordination site of the nickel ion is occupied by an acetonitrile and an oxygen-bound urea molecule. The two ligands were assigned arbitrary positions and occupancies and then refined to the reported positions with 50% occupancy each. All pertinent crystallographic information for each complex, including bond distances and angles, atomic coordinates, and equivalent isotropic displacement parameters, is provided in Tables S1−S15 in the Supporting Information. Selected crystallographic information for the complexes is provided in Table 1.

Kinetics. The decomposition of urea promoted by the dinickel center in complexes **1** and **2** was studied by the method of initial rates. In a typical experiment, an 18 mM solution of **1** in CH_3CN was prepared and serially diluted. The solutions of **1** were incubated at 60 °C for 20 h with swirling at 200 rpm, after which time the ammonia content of the solutions was quantified by using a colorimetric assay reported previously.[28,34] In a control reaction, a solution 20 mM in [Ni(terpy)-$(H_2O)_3$]$(OTs)_2$ and 20 mM in urea was heated and then assayed under the same conditions described above to determine the rate of urea decomposition promoted by a mononuclear nickel species. Another control reaction involved heating 20 mM [$Ni_2(\mu$-OH)(μ-H_2O)(bdptz)-$(H_2O)_2$]$(OTs)_3$ in acetonitrile under the reaction conditions to ensure that none of the ammonia formed resulted from the reaction of the dinickel complex with acetonitrile. No ammonia was detected in either control reaction.

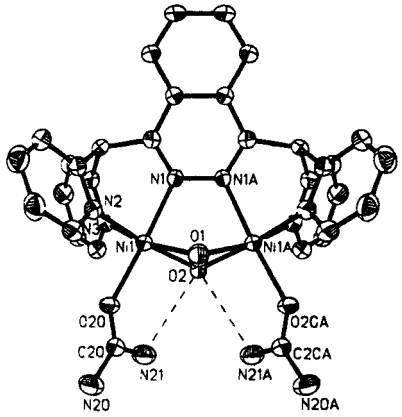

Figure 2. ORTEP diagram of the cation in **1** showing 50% probability ellipsoids for all non-hydrogen atoms. Selected interatomic distances (Å) and angles (degrees): Ni1−O1, 2.204(3); Ni1−O2, 2.060(3); Ni1−O20, 2.027(3); Ni1−N1, 2.044(4); Ni1−N2, 2.079(4); Ni1−N3, 2.072-(4); N21−O2, 2.931(4); Ni1−Ni1A, 3.085(4); N1−Ni1−O20, 171.34-(14); O1−Ni1−O2, 78.37(15).

The rate of cyanate hydrolysis in the presence of **1** was determined for a series of substrate and complex concentrations. When the sodium cyanate concentration was varied from 5 to 24 mM and the concentration of nickel complex was held constant at 11.5 mM, saturation kinetics behavior was observed, indicating coordination of the cyanate to the dinickel complex with a binding constant of 110 ± 30 M^{-1}. The concentration of dinickel complex could not be made sufficiently high to observe saturation when the nickel concentration was varied. When the concentration of the nickel complex was varied from 6 to 14 mM and the cyanate concentration was held constant at 12 mM, the reaction rate showed a first-order dependence on the concentration of dinickel complex. The initial rate of cyanate hydrolysis also had a first-order dependence on the concentration of water in the reaction. The second-order rate constant for this reaction is (9.5 ± 1) × 10^{-4} M^{-1} h^{-1}. When the pH of the reaction was varied from 6.5 to 8.5 by using a buffered solution (0.020 M in HEPES), the rate remained unchanged.

Results

When nickel perchlorate and bdptz are allowed to react with an excess of urea in methanol, complex **1** is obtained. The X-ray crystal structure of **1**, shown in Figure 2, reveals a dinuclear nickel complex bridged by the phthalazine moiety of the bdptz ligand, a water molecule, and a hydroxide ion. Each nickel ion

(30) *SMART*; V5.05 ed.; Bruker AXS, Inc.: Madison, WI, 1998.
(31) Sheldrick, G. M. *SHELXTL: Program for the Refinement of Crystal Structures*; 2nd ed.; University of Gottingen: Gottingen, Germany, 1997.
(32) Sheldrick, G. M. *SADABS: Area-Detector Absorption Correction*; University of Gottingen: Gottingen, Germany, 1996.
(33) Spek, A. L. *PLATON, A Multipurpose Crystallographic Tool*; Utrecht University: Utrecht, The Netherlands, 1998.
(34) Weatherburn, M. W. *Anal. Chem.* **1967**, *39*, 971−974.

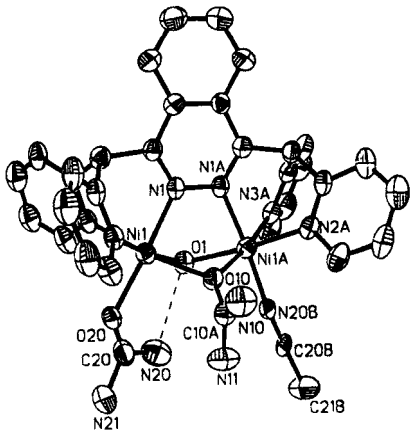

Figure 3. ORTEP diagram of the cation of **2** showing 50% probability ellipsoids for all non-hydrogen atoms. Selected interatomic distances (Å) and angles (degrees): Ni1−O1, 2.039(3); Ni1−O10, 2.158(3); Ni1−O20, 2.14(2); Ni1−N20A, 1.88(3); N20−O1, 2.774(5); Ni1−Ni1A, 3.079(4); Ni−Ni1−O20, 174.2(8); N1−Ni1−N20A, 173.2(10).

is ligated by two pyridine donor arms from the ligand, and the pseudooctahedral coordination sphere of each is filled by a urea molecule bound to nickel through its carbonyl oxygen atom. The electronic spectrum of **1** shows intense $\pi-\pi^*$ transitions below 400 nm, attributable to the ligand and three weak d−d transitions in the visible region, indicating that the nickel ions are in an octahedral environment in solution as well as in the solid state. The solid-state FTIR spectrum of the complex exhibits a shift in the carbonyl stretching frequency of urea from 1690 to 1663 cm^{-1} upon coordination to the dinickel center.

Complex **2** can be obtained through the same reaction as **1** by using acetonitrile as the solvent instead of methanol, or by recrystallizing complex **1** from acetonitrile instead of methanol. An ORTEP diagram of **2** is shown in Figure 3. In this complex, the bdptz ligand coordinates to the dinickel center in the same manner as in complex **1**, with the phthalazine moiety bridging the two metal ions and two pyridine donor arms coordinating to each metal ion. The two remaining terminal coordination positions are each 50% occupied by an acetonitrile molecule and a urea molecule coordinated to the metal through its carbonyl oxygen atom. The dinickel center is additionally bridged by a hydroxide ion and by a urea molecule that forms a single atom bridge between the two metal ions with its carbonyl oxygen atom. The electronic spectrum of **2** confirms the pseudooctahedral coordination environment of the nickel ions in solution. The solid-state FTIR spectrum of **2** is very similar to that of **1**, with the carbonyl stretching bands of the urea molecules producing a somewhat broad peak centered at 1661 cm^{-1}. Comparison of the solution IR spectra of urea and **2** in acetonitrile reveals a shift in the urea stretching frequencies from two sharp peaks at 1712 and 1695 cm^{-1} (C═O stretch and NH_2 bend, respectively) to two much broader peaks at 1660 and 1636 cm^{-1}. Because of the breadth of the peaks and the presence of ligand-derived bands in the same region, it was difficult to distinguish and assign the terminal and bridging urea molecules.

When either complex **1** or **2** is heated to 60 °C in acetonitrile solution, ammonia is produced. The rates of reaction were identical, suggesting that the complexes are the same in solution. Because the initial rates of ammonia production from the two compounds were the same, **1** was used for detailed kinetic studies because it was easier to prepare in satisfactorily pure form. The rate of ammonia production has a first-order dependence on complex concentration, as seen in Figure 4, with

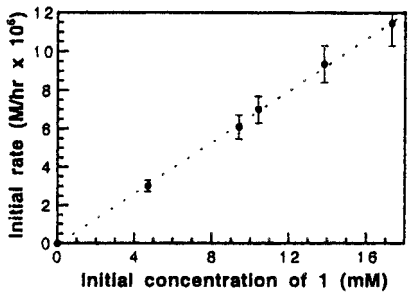

Figure 4. Plot of the initial rate of ammonia formation versus the concentration of **1**.

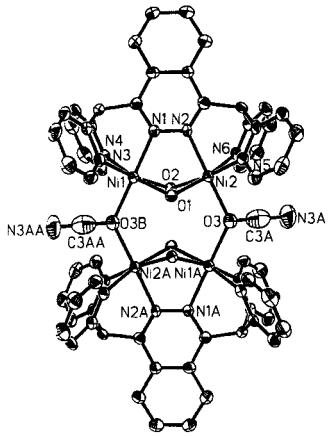

Figure 5. ORTEP diagram of the cation of **3** showing 50% probability ellipsoids for all non-hydrogen atoms. Selected bond lengths (Å) and angles (degrees): Ni1−O1, 2.123(3); Ni1−O2, 2.091(3); Ni1−O3B, 2.050(4); Ni2−O1, 2.109(3); Ni2−O2, 2.088(3); Ni2−O3, 2.050(3); Ni1−Ni2, 3.048(4); N1−Ni1−O3B, 179.52(15); N2−Ni2−O3, 178.85-(13); O3−C3A−N3A, 179.3(9).

an observed rate constant of $(7.7 \pm 0.5) \times 10^{-4}$ h^{-1}. When urea, alone or with added $[Ni(terpy)(H_2O)_3](OTs)_2$, was heated under the same conditions in acetonitrile, no ammonia was produced, indicating that two metal ions act in concert to effect the decomposition of urea at least 500 times faster than the spontaneous decomposition of urea under these conditions. The dinickel complex promotes the decomposition of urea to ammonia and cyanate rather than the hydrolysis of urea to ammonia and carbamate, as evidenced by the presence of a strong cyanate band in the FTIR spectrum of the reaction product.

Although attempts to obtain X-ray quality crystals of the cyanate-containing product were unsuccessful, an analogue was synthesized independently by allowing $[Ni_2(\mu\text{-OH})(\mu\text{-}H_2O)(bdptz)(H_2O)_2](OTs)_3$ to react with 1 equiv of NaNCO in aqueous ethanol. Green X-ray quality crystals of this cyanate complex, $[Ni_2(\mu\text{-OH})(\mu\text{-}H_2O)(bdptz)(\mu\text{-OCN})]_2(OTs)_4$, **3**, were harvested following slow evaporation of the solvent from the reaction mixture. An ORTEP diagram of **3** is displayed in Figure 5. Complex **3** consists of two dinuclear nickel units, each bridged by the phthalazine moiety of bdptz and ligated by its pyridine donor arms, with a water molecule and a hydroxide ion filling the two remaining bridging positions. Two cyanate ions link the two dinickel units, each bridging through its oxygen atom. The bridging atom can clearly be assigned as oxygen on the basis of crystallographic data. When the structure was refined with nitrogen assigned as the bridging atom, the U_{eq} values for the oxygen and the nitrogen atom increased and decreased by over 50%, respectively. Further evidence for the assignment of the bridging atom as oxygen is provided by the cyanate bond

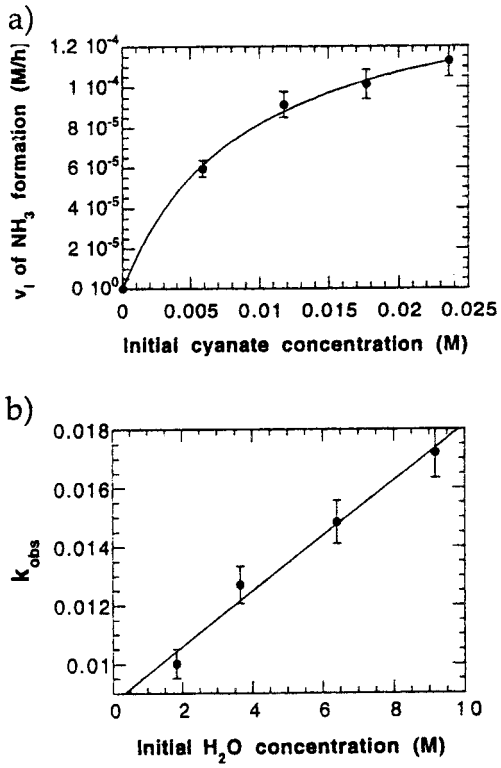

Figure 6. Plots showing (a) the dependence of the initial rate of cyanate hydrolysis on the initial concentration of $[Ni_2(OH)(H_2O)_3(bdptz)](OTs)_3$ and (b) the dependence of the observed rate constant of cyanate hydrolysis (h^{-1}) on the concentration of water in the reaction mixture.

lengths. The O−C distance of 1.290(14) Å is slightly longer than that in other cyanate complexes, and the C−N distance is 1.149(14) Å, just shorter than the average distance in known cyanate complexes. A slight lengthening of the C−O bond accompanied by a similar shortening of the C−N bond would be expected in an oxygen-bound cyanate complex, corresponding to increased negative charge on the bridging oxygen atom and a strengthening of the C−N bond. Both the solution and solid-state FTIR spectra of **3** are virtually identical to that of the reaction product. The ν_{as} of cyanate occurs at 2164 cm^{-1} in both cases.

When either **1** or **2** was heated in a 50% aqueous acetonitrile solution, ammonia was produced at a rate comparable to that in dry acetonitrile but with no appreciable buildup of the cyanate-containing product. This result indicates that the cyanate-containing product is hydrolyzed in the presence of water. Further evidence to support this hypothesis was obtained by first heating **1** in dry acetonitrile for several days to allow the cyanate product to accumulate, then adding several equivalents of water, and observing the characteristic cyanate peak in the IR spectrum decrease over time. Cyanate hydrolysis was followed quantitatively by allowing sodium cyanate to react with the hydroxide-bridged dinickel complex $[Ni_2(\mu\text{-}OH)(\mu\text{-}H_2O)(bdptz)(H_2O)_2](OTs)_3$. The reaction exhibited saturation kinetics behavior as the concentration of cyanate ion was varied. A binding constant of 110 ± 30 M^{-1} for coordination of cyanate to the dinickel complex was obtained from the data, as shown in Figure 6a. The reaction has a first-order dependence on the concentration of water, as indicated in Figure 6b, with a second-order rate constant of (9.5 ± 1) × 10^{-4} M^{-1} h^{-1}. When the pH of the reaction was varied from 6.5 to 8.5, the rate was unaffected.

Discussion

In both complexes **1** and **2**, there are two nickel ions in pseudooctahedral ligand environments, a geometry imposed in part by the hexadentate, dinucleating bdptz ligand. Both complexes contain two coordinated urea molecules and a bridging hydroxide ion that could potentially serve as a nucleophile for substrate hydrolysis. The coordination of urea to the dinuclear nickel centers in **1** and **2** reinforces the proposal that urea most likely binds preferentially through its carbonyl oxygen atom to an active site nickel center in urease. The bridging coordination mode of urea in complex **2** has not previously been encountered and may be of relevance to the enzyme. Presumably, the urea molecule would be better activated by coordination to two metal ions rather than just one. In the urea decomposition chemistry reported here, however, it is unknown which binding mode facilitates the elimination reaction.

It is interesting to speculate why in the present work the urea molecule undergoes an elimination reaction rather than being hydrolyzed. We recently reported the hydrolysis of picolinamide by an analogous hydroxide-bridged dinickel complex;[28] in this case, intramolecular nucleophilic attack of the bridging hydroxide ion resulted in hydrolysis of a coordinated amide. Since **1** and **2** both contain such a bridging hydroxide ion, why does intramolecular nucleophilic attack not occur? Perhaps the hydroxide ion, although able to effect the hydrolysis of an amide substrate, is not sufficiently nucleophilic to hydrolyze the coordinated urea molecule. Another possibility is that the coordinated hydroxide ion serves as a general base, aiding in the deprotonation of urea to favor elimination. The terminally coordinated urea molecule in both **1** and **2** is hydrogen bonded through one of its amino groups to the bridging hydroxide ion (Figures 2 and 3), providing a facile pathway by which the hydroxide ion could participate in such a reaction.

The products of the reaction between urea and the dinuclear nickel complex are ammonia and cyanate. Attempts to crystallize the cyanate-containing product afforded crystals too small to be characterized by X-ray crystallography, but the IR spectrum of these crystals closely resembled that of the independently synthesized cyanate complex **3**. It is difficult to distinguish between bridging and terminally coordinated cyanate on the basis of ν_{CN},[35] and the other cyanate bands are obscured by ligand vibrations. Although there is insufficient evidence to demonstrate that **3** is the same as the product formed upon decomposition of bound urea in **1** or **2**, the similarities in the spectra and properties indicate **3** to be a reasonable candidate for the urea decomposition product.

The cyanate product formed upon heating complexes **1** or **2** can be further decomposed hydrolytically in the presence of water. This hydrolysis reaction was quantitated by following the hydrolysis of NaNCO by $[Ni_2(\mu\text{-}OH)(\mu\text{-}H_2O)(bdptz)(H_2O)_2](OTs)_3$. As the concentration of cyanate was varied, saturation kinetics were observed. The calculated nickel−cyanate binding constant was 110 ± 30 M^{-1}. The concentration of the nickel complex could not be made sufficiently high to observe saturation behavior when the nickel concentration was varied. Under these reaction conditions, the rate showed a first-order dependence on the concentration of dinickel complex. The reaction rate was also first-order in water, indicating that the hydrolysis proceeds by attack of an external water molecule on the coordinated cyanate ion. The pH independence of the reaction in the range 6.5 ≤ pH ≤ 8.5 indicates that the bridging

(35) Bailey, R. A.; Kozak, S. L.; Michelsen, T. W.; Mills, W. N. *Coord. Chem. Rev.* **1971**, *6*, 407−445.

Scheme 2

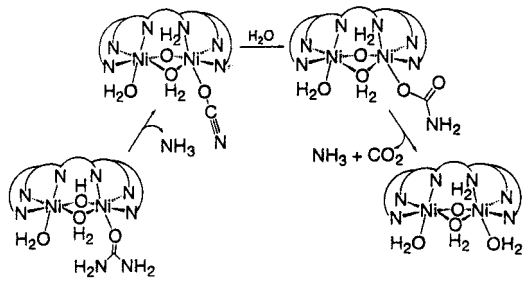

hydroxide ion could be acting as a general base in this reaction, helping to deprotonate the external nucleophile. The pK_a of this bridging hydroxide ion is 4.4,[28] well below 6.5.

The net reaction effected at the dinickel center is hydrolysis of urea to ammonia and carbon dioxide through formation of a cyanate intermediate. This reaction proceeds via a pathway distinct from that previously proposed for the enzymatic hydrolysis of urea (Scheme 1).[1,7,9c] As shown in Scheme 2, the important steps in the hydrolysis of urea at the dinickel center in **1** and **2** are (i) elimination of ammonia from the coordinated urea molecule, and (ii) hydrolysis of the resulting cyanate by an external water molecule. Coordination of urea to the dinuclear nickel center is crucial; complexes **1** and **2** promote the elimination of ammonia from coordinated urea at a rate at least 500 times as fast as the reaction between urea and a mononuclear nickel complex or urea alone. The final hydrolysis step is significant. Other researchers have reported the formation of cyanate from urea at a dinickel site but have not investigated the reactivity of the resulting cyanate complex. To the best of our knowledge, there is no definitive evidence ruling out the possibility of a transient nickel-bound cyanate intermediate in urease. Such an intermediate would be consistent with the results of the present and other model studies.[25−27]

Acknowledgment. This work was supported by grants from the National Science Foundation and the National Institutes of Health. A.M.B. thanks the NIH for a predoctoral fellowship. We thank Dr. Natalia Kaminskaia for helpful discussions.

Supporting Information Available: Figures S1−S3, showing fully labeled ORTEP diagrams for complexes **1**−**3**, respectively. Figure S4 shows the nickel complex concentration dependence of the initial rate of cyanate hydrolysis, and Figure S5 shows the pH independence of the rate over the range 6.5−8.5 (PDF). X-ray crystallographic files, in CIF format, are available on the Internet only. This material is available free of charge via the Internet at http://pubs.acs.org.

JA000202V